

Mineralogical analysis of a residual soil from Medellín Dunite (Colombia) and its influence on physical properties and unsaturated undrained shear strength

Victoria Meza-Ochoa^{1*} ; Álvaro L. Morales² 
Marco Antonio Márquez-Godoy³ 

¹Grupo de Investigación en Ingeniería Sostenible (GIS), Facultad de Ingeniería, Politécnico Colombiano Jaime Isaza Cadavid, Medellín, Colombia. (*) vemeza@elpoli.edu.co

²Grupo de Estado Sólido, Instituto de Física, Universidad de Antioquia, Medellín, Colombia. amoral@fisica.udea.edu.co

³Grupo de Mineralogía Aplicada y Bioprocesos, Facultad de Minas, Universidad Nacional de Colombia, sede Medellín, Colombia. mmarquez@unal.edu.co

Abstract

The residual soils have a physical-mechanical behavior that reflects their formation process. In the present work, a residual soil derived from Medellín Dunite was characterized mineralogically and its influence on the physical properties and unsaturated undrained shear strength was evaluated. The samples were taken in the area adjacent to “Canteras de Colombia”, in Bello municipality (Antioquia, Colombia), on the east side of the Medellín-Bogotá highway. To obtain a relationship between mineralogy and physical-mechanical properties, mineralogical characterization with X-ray diffraction (XRD), Fourier transform infrared spectroscopy (FTIR), and Mössbauer spectroscopy was done to determine the mineral phases present at three depths above 1.80 m in a soil profile derived from Medellín Dunite. The index properties and undrained shear strength of these soils were determined, the latter by the unconfined compressive strength (UCS) test and unconsolidated-undrained (UU) triaxial compression test. The residual soils of Medellín Dunite, have a particular mineralogical composition, which has a significant bearing on their physical-mechanical behavior. The more superficial soils (0.00 a 0.30 m) are richer in iron oxides and hydroxides (hematite, maghemite, and goethite) and aluminum hydroxides (gibbsite), forming bonds between the particles that produce soil aggregation. They are of lateritic behavior and fragile, and present, more significant cohesion and larger undrained shear strength than deeper soils (0.30 m to 1.80 m), these present lower content of oxides and oxi-hydroxides and higher content of silicates like clinocllore and tremolite.

Keywords: Medellín Dunite; Mineralogy of dunite residual soils; Lateritic soils; Oxides and oxi-hydroxides; Unsaturated undrained shear strength.

Análisis mineralógico de un suelo residual de la Dunita de Medellín (Colombia) y su influencia en las propiedades físicas y la resistencia al corte no drenada de suelos no saturados

Resumen

Los suelos residuales presentan un comportamiento físico-mecánico que es el reflejo de su proceso de formación. En la presente investigación, un suelo residual derivado de la Dunita de Medellín fue caracterizado mineralógicamente, y se evaluó su influencia en algunas propiedades físicas y en la

How to cite: Meza-Ochoa, V.; Morales, A.L.; Márquez-Godoy, M.A. (2023). Mineralogical analysis of a residual soil from Medellín Dunite (Colombia) and its influence on physical properties and unsaturated undrained shear strength. *Boletín de Geología*, 45(1), 87-101. <https://doi.org/10.18273/revbol.v45n1-2023004>

resistencia al corte no drenada en condición no saturada. Los suelos estudiados se localizan en el sector contiguo a “Canteras de Colombia”, en el municipio de Bello (Antioquia, Colombia), sobre el costado oriental de la autopista Medellín-Bogotá. En la zona de estudio, se seleccionó un talud y se tomaron muestras del suelo a diferentes profundidades (por encima de 1,8 m) dentro del perfil de meteorización. La caracterización mineralógica para determinar las fases minerales presentes en los suelos se hizo utilizando difracción de rayos X (DRX), espectroscopía infrarroja por transformada de Fourier (FTIR) y espectroscopía de Mössbauer. Fueron determinadas las propiedades índice del suelo y la resistencia al corte no drenada, esta última mediante los ensayos de resistencia a la compresión no confinada (UCS) y resistencia a la compresión triaxial no consolidada-no drenada (UU). Los suelos residuales derivados de la Dunita de Medellín presentan una composición mineralógica particular, que al parecer tiene un efecto significativo en su comportamiento físico-mecánico. Los suelos más superficiales (0,00 a 0,30 m) se encuentran enriquecidos en óxidos y oxi-hidróxidos de hierro (hematita, magemita y goetita) e hidróxidos de aluminio (gibbsite), formando enlaces entre-partículas que producen agregación a los suelos. Estos son de comportamiento laterítico y frágil, y presentan mayor cohesión y mayor resistencia al corte no drenada que los suelos residuales de los horizontes más profundos (0,30 m a 1,80 m), que a su vez presentan menor contenido de óxidos y oxi-hidróxidos y mayor contenido de silicatos como clinocloro y tremolita.

Palabras clave: Dunita de Medellín; Mineralogía de suelos residuales de dunita; Suelos lateríticos; Óxidos y oxihidróxidos; Resistencia al corte no drenada de suelos no saturados.

Introduction

Some dense urban settlements of the city of Medellín (Antioquia) and its surroundings were developed in areas where the geologic body called “Medellín Dunite” is located. There is particular interest in the study of dunite residual soils, due to several catastrophic events associated with landslides, which have claimed the lives of hundreds of human beings and damaged homes. Among the most important, are i) the Media Luna landslide (12 July 1954, 70 deaths); ii) the Santo Domingo landslide (29 September 1974, 50 deaths); iii) the Villatina landslide (27 September 1987), where more than 500 people died and more than 100 homes were destroyed, buried by 20000 m³ of soil and rock; and iv) the Gabriela landslide (5 December 2010, 83 deaths) (Serna-Quintana, 2011). In this sense, it is necessary to study the behavior of these soils, with the aim that the results shed light on the behavior associated with the problems of instability.

The Medellín Dunite, more recently named by Garcia-Casco *et al.* (2020) as the “Medellín Metaharzburgitic Unit”, is a cretaceous igneous unit (possibly between the Triassic and the early Cretaceous) (Álvarez-Agudelo, 1987). This unit with about 70 km² of area crosses the Medellín river valley (called “Aburrá Valley”), in an N10°W direction, going from the Envigado municipality up to the south of the San Pedro municipality (Figure 1). The rocks are mainly constituted by olivine and pyroxene as a primary mineral phase and an extremely rare presence of diopside, augite. They show a variable extent of

serpentine-group minerals replacement (lizardite, antigorite, chrysotile) and iddingsite (a mixture of fine-grained chlorite group and smectite group minerals with iron oxi-hydroxides). They were also reported as minor and accessory minerals: magnetite, chromian-spinel, ferrian-chromite, amphiboles (tremolite), sulfides, etc. (Garcia-Casco *et al.*, 2020).

The residual soils generated from Medellín Dunite reach thicknesses between 10-40 m. Rigidity is highly variable, but generally, the penetration resistance gradually increases with depth, except for surface horizons (lateritic crust) with high iron content (iron oxides with oolitic and botryoidal habits) (Rodríguez *et al.*, 2005).

The relationship between the mineralogy and the geotechnical properties of soils has focused mainly on the study of the clay minerals and their effects on resistance (Tsige and González de Vallejo, 1996; Shaqour *et al.*, 2008) and volume changes (Fookes, 1997; Rahardjo *et al.*, 2004). Other research has focused on studying the effect of weathering on the geotechnical properties of soils and rocks (Bo *et al.*, 2015).

In Medellín, several studies of mineralogical and physical characterization of soils derived from other geological formations have been carried out, such as those on residual soils of the Antioquian Batholith (Romaña *et al.*, 2009) and lateritic soils derived from amphibolite (Fresneda-Saldarriaga *et al.*, 2013), however, no study was reported on the soils derived from dunite.

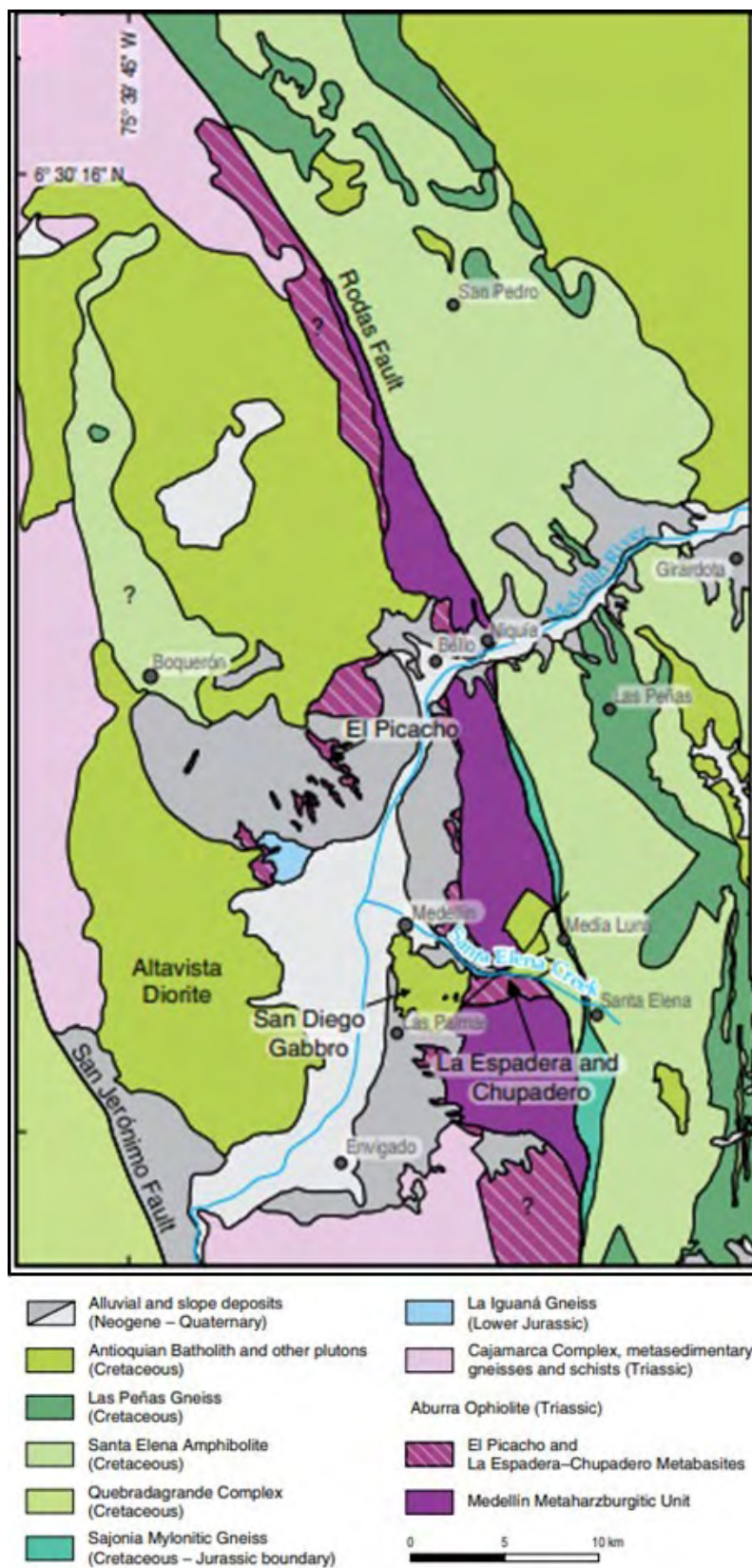


Figure 1. Simplified geological map of the Medellín region, showing the “Medellín Dunite” or “Medellín Metaharzburgitic Unit”. Adapted from García-Casco *et al.* (2020).

This article presents the results of the mineralogical characterization of residual soil from “Medellín Dunite” and its relationships with the physical properties and unsaturated undrained shear strength.

Methods

The residual soils were taken in Bello municipality (Antioquia, Colombia), on the east side of the Medellín - Bogotá highway, in the area adjacent to “Canteras de Colombia”, localized at the geographic coordinates of 6.318895 Latitude, -75.545899 Longitude (Figure 2) and a height of 1595 m above mean sea level (AMSL).

A typical slope (4 m high) was chosen, where the samples were taken at different depths, using percussion

drilling equipment. Three boreholes were made in the slope area to obtain the soil samples. Disturbed samples were recovered with a split spoon sampler, and undisturbed samples with a Shelby sampler.

On the slope cut, three weathering horizons were visually differentiated according to macroscopic characteristics like the color and texture changes, in the following way: i) H-1 horizon, the most superficial horizon in the range 0.00 and 0.30 m, ii) H-2 horizon, intermediate horizon between 0.30 and 0.80 m, iii) H-3 horizon, in the range 0.80 to 1.80 m. The weathering profile was classified according to the system proposed by Little (1969) and according to Deere and Patton (1971).



Figure 2. Study area. A. Map of Colombia (Geoportál IGAC). B. Slope location (Google map© image 2022). C. Slope cut photography.

Mineralogical characterization

The mineralogical characterization was done using X-ray diffraction (XRD), Fourier transform infrared spectroscopy (FTIR), and Mössbauer spectroscopy. For this purpose, the samples were disaggregated manually, ground in an agate mortar, and sieved through 200 Tyler mesh. The XRD measurement was done in a MiniFlex™ II Rigaku diffractometer, using a Cu cathode tube, with a 30 kV accelerating voltage, with a current of 30 mA, doing a scanning between 5-70° 2 θ , in a step-by-step mode, using a 0.02° step and 2 s per step. X'Pert High Score Plus and Jade software were used for the spectra analysis. FTIR analyses were done, with a Shimadzu (FTIR 8400S) spectrometer, using a transmission mode, in a 400 to 4000 cm⁻¹ range, 24 scans, and a Happ-Genzel apodization. For the analysis, KBr pellets were prepared, 1 mg of sample and 100 mg KBr, pressed to 10 t. FTIR spectra were interpreted using IR-solution software. Finally, Mössbauer spectroscopy analyses were made using a Wissel spectrometer, in a transmission mode, with a ⁵⁷Co (Rh matrix) source, at room temperature. The spectra analysis was made using the software Recoil® (Lagarec and Rancourt, 1998). Disturbed soil samples were used for these tests, selecting a single representative sample from each horizon.

Physical characterization and undrained shear strength

The index properties of the soils were established through tests of natural moisture content (ω), specific gravity (G_s), and Atterberg's limits, following the ASTM D854-14, ASTM D4318-17e1 and ASTM D2216-19 standards. For these tests, three representative samples of each horizon are used and the results presented correspond to the average value obtained in the tests. The particle size distribution was determined by mechanical sieving and hydrometer (ASTM D422-63(2007)e1). Also, laser granulometry tests were made using a particle size analyzer Mastersizer, Model S, Malvern Instrument Ltda. In addition, measures were made of the soil pH in water and potassium chloride (KCl) to determine the Δ pH, as an indication of the dominant minerals (Kiehl, 1979).

In addition, the soils were classified by the Unified Soil Classification System (USCS) (ASTM D2487-17e1) and by the Miniature Compacted Tropical (MCT) methodology (Nogami and Villibor, 1994). The MCT classification was implemented in Brazil to identify the presence of lateritic soils, characteristic of some tropical environments.

The undrained shear strength of soils was evaluated by the unconfined compressive strength (UCS) test (ASTM D2166-16) and unconsolidated-undrained (UU) triaxial compression test (ASTM D2850-15) performed on cylindrical undisturbed specimens (5 cm diameter and 8.9 cm height). The UU triaxial test was carried out on unsaturated samples, using confining pressures of 50, 100, and 200 kPa.

Results and discussion

Description of the weathering profile

From the macroscopic features of the slope cut, three horizons were identified within the weathering profile. According to Little's classification (1969), the three horizons identified to form part of the "residual soil" (grade VI of weathering), and according to the classification proposed by Deere and Patton (1971), they have been classified within horizon I "residual soil", and are discriminated as:

- Horizon H-1 (0.00 – 0.30 m): residual soils of the horizon IB, with silty texture, color bright brown (7.5 YR 5/8) according to the Munsell color system, and hard consistency in dry condition (National Engineering Handbook, 2021).
- Horizon H-2 (0.30 – 0.80 m): residual horizon in the transition between horizons IB and IC, silty texture, strong brown color (7.5 YR 5/8), and hard consistency in dry condition (National Engineering Handbook, 2021).
- Horizon H-3 (0.80 – 1.80 m): saprolite, horizon IC, silty texture, strong brown color (7.5 YR 5/8) with black and reddish mottles, and hard consistency in dry condition (National Engineering Handbook, 2021).

Mineralogical characterization

XRD results showed the occurrence of goethite and clinocllore (probably chamosite) as major phases; while gibbsite, kaolinite, talc, and tremolite, as minor phases. In addition, some traces of maghemite and possible hematite reveal differences in contents and mineralogy between the horizons (Figure 3).

The H-1 horizon showed the dominance of goethite, with minor contents of gibbsite, clinocllore (chamosite), kaolinite, talc, and traces of maghemite and possibly hematite. In the H-2 horizon, the

difference was a goethite content decrease and an increase in the clinocllore, with minor diminution in the talc, gibbsite, and possibly kaolinite. The H-3 horizon revealed a clear predominance of clinocllore, with the appearance of tremolite, a significant

decrease in the content of goethite and kaolinite, and the disappearance of talc and gibbsite. However, it is essential to mention that goethite and gibbsite were observed as low crystallinity phases, evidenced by broad and poorly defined peaks (Figure 3).

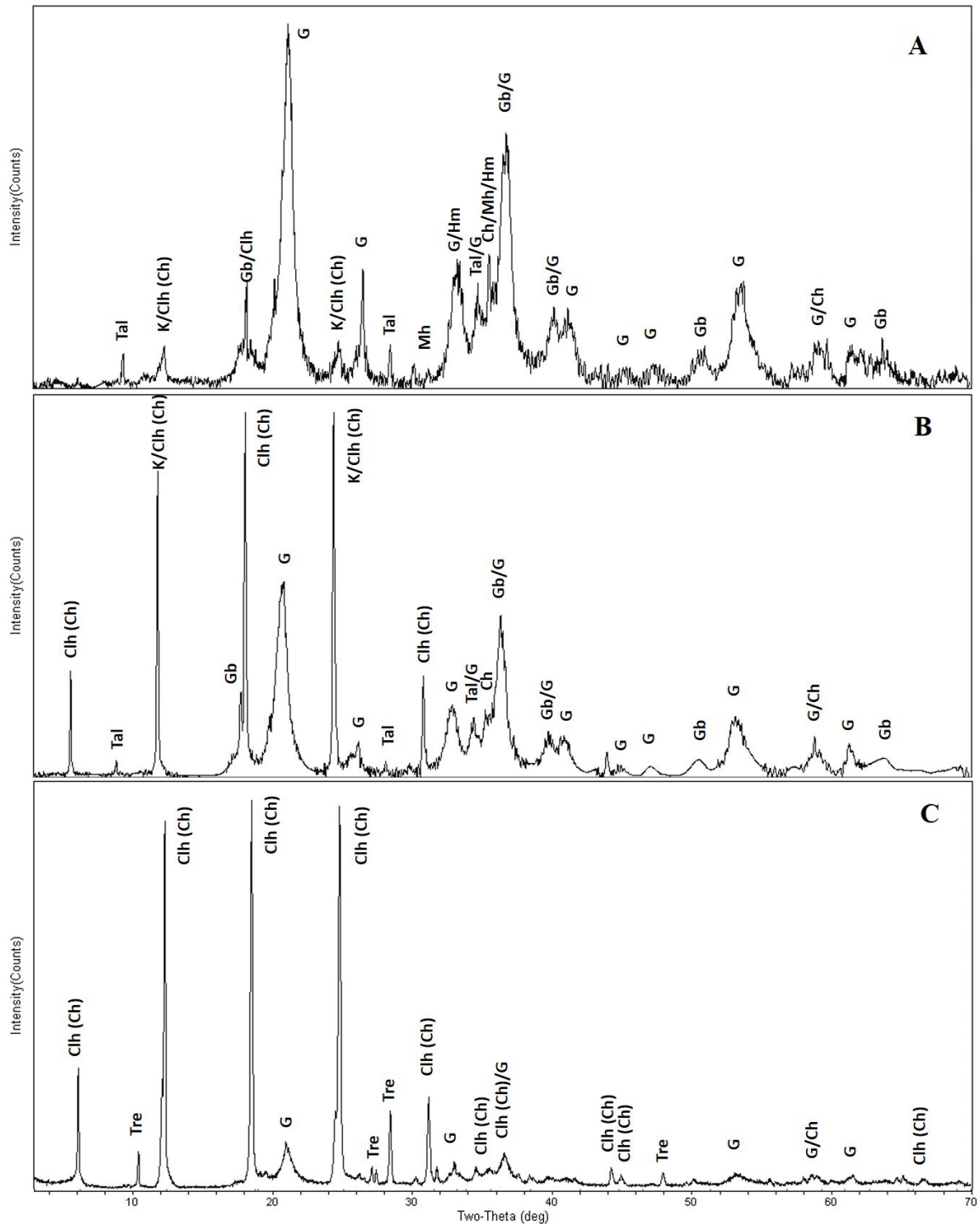


Figure 3. X-ray diffraction for the horizons. **A.** H-1, **B.** H-2, and **C.** H-3. Note: Clh (clinocllore), Ch (chamosite), Tre (tremolite), G (goethite), K (kaolinite), Gb (gibbsite), Tal (talc), Mh (maghemite) and Hm (hematite).

By the FTIR analysis (Figure 4) was evident the occurrence of goethite, clinocllore, kaolinite, gibbsite, hematite/maghemite, and possibly talc (overlapping bands with kaolinite) (bands at 3676 cm⁻¹, 3654 cm⁻¹, 1015 cm⁻¹, and 466 cm⁻¹). The FTIR results, confirm the occurrence of kaolinite in H-1, H-2, and, in traces, in the H-3 horizon, not so apparent by XRD, due to the overlap of its principal peaks with the clinocllore. Soil samples fractions sieved of the pass 200 (P) and retained 200 (R) Tyler mesh do not show any dissimilarity for the different horizons.

Furthermore, the XRD and FTIR analyses showed differences in the mineralogy of the horizons, with

a predominance of gibbsite and goethite in the H-1, kaolinite and gibbsite in H-2, in contrast to the mineralogy of the H-3 horizon, where there is a prevalence of clinocllore.

Figure 5 and Table 1 show the results of the Mössbauer analysis. Figure 5A shows a Mössbauer spectrum of H-1, the uppermost horizon, where two sextets for hematite and maghemite and three doublets corresponding to goethite, were observed and clinocllore (possibly minor kaolinite). Mössbauer spectra of the horizons H-2 and H-3, shown in Figures 5B and 5C, present a decrease of the sextets of hematite and maghemite and an increase of the doublet of goethite/clinocllore.

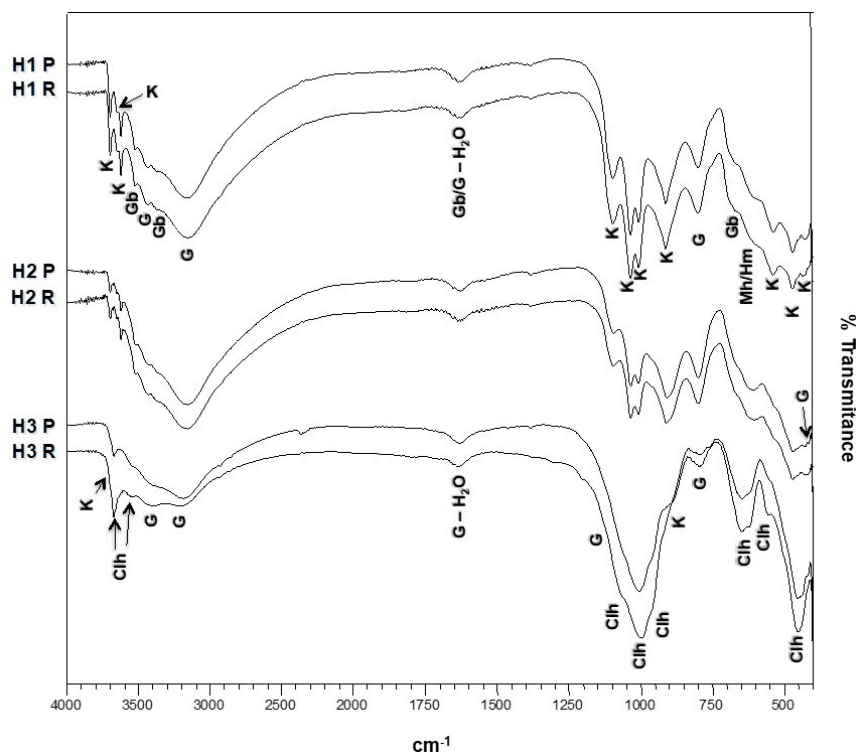


Figure 4. FTIR spectra for the horizons H-1, H-2, and H-3. Note: P: pass sieve No 200; R: retained sieve No 200. Clh (clinocllore), G (goethite), K (kaolinite), Gb (gibbsite), Mh (maghemite) and Hm (hematite).

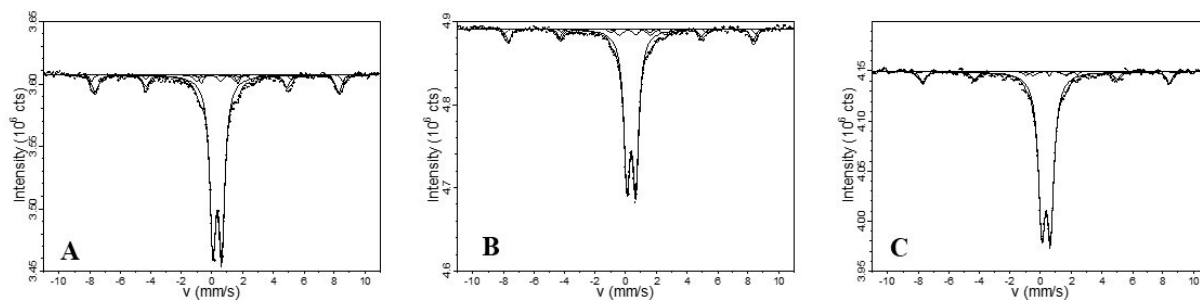


Figure 5. Mössbauer spectra for the A. H-1, B. H-2, C. and H-3 horizons.

The doublet 1 is assigned, at least in part, to superparamagnetic goethite, with a mean particle size below 13 nm (Morales, 2003). The doublet 1 contains contributions from goethite and clinochlore and its combined percentage abundance stays relatively constant in going from H-1 to H-3, i.e., from 74%

to 84%. In H-1, doublet 1 is dominated by goethite, and in H-3 clinochlore dominates (see Figure 4), this behavior shows that one component grows at expense of the other component, which is related to the iron content of both clinochlore and the iron oxides.

Table 1. Mössbauer parameters for H-1, H-2, and H-3 horizons.

| Horizons | ^a CS (± 0.01) (mm/s) | ^b Δ (± 0.01) (mm/s) | ^c B(T) (±0.01) | Area (%) (± 2) | ^d Mineral |
|------------|------------------------------------|-----------------------------------|------------------------------|-------------------|----------------------|
| H-1 | | | | | |
| Doublet 1 | 0.46 | 0.58 | | 74 | G, Clh-K |
| Doublet 2 | 0.61 | 2.40 | | 3 | K |
| Doublet 3 | 1.71 | 2.10 | | 2 | K |
| Sextet 1 | 0.48 | -0.04 | 50.91 | 4 | Hm |
| Sextet 2 | 0.41 | 0.01 | 49.34 | 17 | Mh |
| H-2 | | | | | |
| Doublet 1 | 0.48 | 0.57 | | 78 | G, Clh-K |
| Doublet 2 | 0.71 | 2.10 | | 4 | K |
| Doublet 3 | 1.71 | 1.90 | | 3 | K |
| Sextet 1 | 0.51 | -0.1 | 50.82 | 4 | Hm |
| Sextet 2 | 0.43 | 0.01 | 49.55 | 11 | Mh |
| H-3 | | | | | |
| Doublet 1 | 0.48 | 0.57 | | 84 | G, Clh-K |
| Doublet 2 | 0.71 | 2.20 | | 2 | K |
| Doublet 3 | 1.61 | 1.80 | | 1 | K |
| Sextet 1 | 0.51 | -0.05 | 51.59 | 1 | Hm |
| Sextet 2 | 0.46 | 0.01 | 49.93 | 12 | Mh |

Note: ^aCS: chemical shift, ^bΔ: splitting, ^cB(T): magnetic field (teslas)
^dG (goethite), Clh-K (clinochlore with possibly minor kaolinite), K (kaolinite), Mh (maghemite) and Hm (hematite)

These results are in agreement with the measurements from XRD and FTIR discussed above. Also, the goethite abundance percentage grows, from the H-3 sample to the H-1 sample, at expense of the decrease of the magnetic part, hematite plus maghemite, and also due to the clinochlore weathering. Kaolinite is present only in small quantities, due to the small iron content, and decreases as goethite increases, but this is not evident from Mössbauer spectroscopy since its amount is close to the area error.

The results of the mineral characterization show for H-1 a larger relative quantity of goethite, gibbsite, and

iron oxides (hematite, maghemite) which decrease with increasing depth (H-2, H-3) and decreasing weathering, while clinochlore increases with increasing depth. These minerals, goethite, gibbsite, and iron oxides, can act as cementitious material and generate particle aggregations in the soil, especially gibbsite due to the presence of free cations at one of its tetrahedral sites (Araki, 1997).

Physical characterization

Table 2 shows the results of the physical characterization of Medellín Dunite residual soils for the horizons H-1, H-2, and H-3.

Table 2. Physical characterization of Medellín Dunite residual soils.

| Properties | H-1 | H-2 | H-3 |
|--|------|------|------|
| Water content, ω % | 37 | 43 | 52 |
| % Sand | 25 | 14 | 12 |
| % Fines, size smaller than 75 μm | 75 | 86 | 88 |
| % Clay fraction particles < 0.005 mm | 61 | 62 | 62 |
| Liquid Limit, LL (%) | 49 | 62 | 72 |
| Plasticity Index, PI (%) | 8 | 17 | 15 |
| Void ratio, e | 1.2 | 1.4 | 1.8 |
| Dry density, γ_d (kN/m ³) | 14.8 | 13.3 | 11.8 |
| Specific gravity, Gs | 3.24 | 3.22 | 3.24 |
| *USCS | ML | MH | MH |
| **MCT | LG' | NS' | NS' |

Note: *USCS: Unified Soil Classification System: ML, medium plasticity silts MH, high plasticity silts
 **MCT: Miniature Compacted Tropical: LG', laterite clay silt NS', not lateritic silt

Grain size distribution and Atterberg's limits: The results of the granulometric analysis showed that the dunite residual soils studied were fine-grained soils, with fines content greater than 75% and sand content between 12% - 25%. The H-1 horizon has the lowest fines content (75%) compared to the H-2 and H-3 horizons (86%, 88%). As the fines content increases with depth, the liquid limit (LL), plastic limit (PL), and plasticity index (PI) increase with depth (Figure 6).

The H-1 horizon presents LL= 49% and PI= 8%, while soils H-2 and H-3 have larger values of LL, between 62% and 72%, and PI between 15% and 17%.

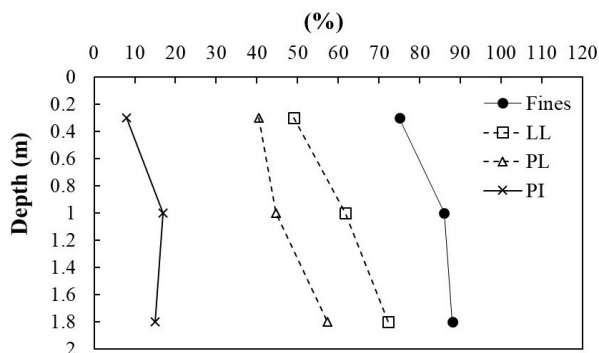


Figure 6. Soil profile, Atterberg's limits, and fines fraction of Medellín Dunite residual soils.

Casagrande's chart (Figure 7) shows that soils H-1, H-2, and H-3 are located below A-line (silty soils)

and on the right side, in the high plasticity area of the graph. However, each horizon location within the chart is different, representing possible differences in mineralogy and therefore, in physical-mechanical behavior.

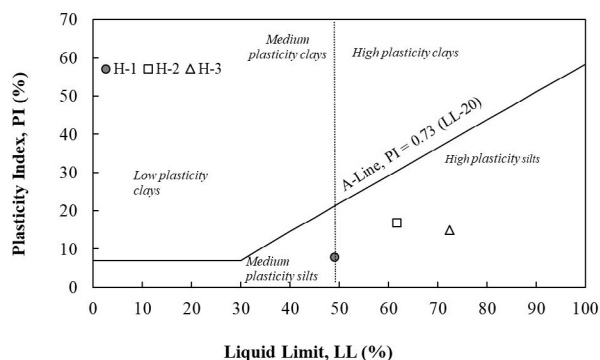


Figure 7. Casagrande's chart, horizons H-1, H-2, H-3 of Medellín Dunite residual soils.

To analyze interparticle aggregation, laser granulometry tests were carried out with and without dispersant, using sodium hexametaphosphate. The results showed high variability in the grain size distribution when it is determined with and without dispersant. This behavior is more pronounced in H-1 (Figure 8) evidencing lower structural stability of these soils to chemical agents and a higher content of aggregates (Araki, 1997).

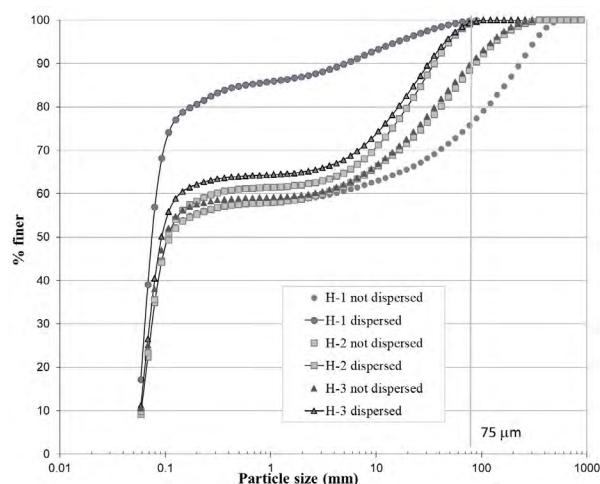


Figure 8. Particle size distribution for the horizons H-1, H-2, and H-3, of Medellín Dunite residual soils, with and without dispersant.

The total aggregates percentage (AT) defined by Araki (1997) is shown in Table 3, with a value of AT=21% in the H-1 horizon, a greater value than the total aggregates of the H-2 and H-3 horizons, which presented the same value of AT=6%.

A higher percentage of aggregation in H-1 could be due to a higher content of minerals acting as cementing agents, which disintegrate when they come into contact with the dispersant.

The upper horizon H-1 presents a more significant aggregation of particles and a greater sensitivity of its structural stability towards chemical agents such as sodium hexametaphosphate. This particle aggregation could be associated with an important mineral presence (goethite, gibbsite, and iron oxides), which acts as cementitious material and interparticle bond.

Table 3. Total aggregates according to Araki (1997).

| Properties | H-1 | H-2 | H-3 |
|--|-----|-----|-----|
| % Fines (size smaller than 75 μm) without dispersant | 75 | 86 | 88 |
| % Fines (size smaller than 75 μm) with dispersant | 96 | 92 | 94 |
| ^a AT = % Fines (with dispersant) - % Fines (without dispersant) | 21 | 6 | 6 |

Note: ^aAT: total aggregates

USCS and MCT soil classification: Based on the results of grain size and plasticity, the H-1 horizon was classified as ML, medium plasticity silts, and samples of the H-2 and H-3 horizons were classified as MH, high plasticity silts, according to the USCS.

From the MCT methodology, the H-1 horizon was classified as laterite clay silt (LG'), and samples of the H-2 and H-3 horizons were classified as not lateritic silt (NS'). The first 30 cm of soil (horizon H-1) shows a concentration of iron and aluminum oxides, which according to Gidigasú (1972) is evidence of laterization, very different from the H-2 and H-3 horizons, which are non-lateritic.

On the other hand, the calculated ΔpH for the three horizons gave positive values in the range of 0.3-1.1 (Table 4), which indicates the dominance of iron oxi-hydroxides (Kiehl, 1979), in agreement with the mineralogical characterization. The lateritic horizon H-1 shows the highest value of ΔpH (1.1) compared to the non-lateritic horizons H-2 and H-3 (0.3, 0.7).

Table 4. pH measurements of Medellín Dunite residual soils.

| Horizon | pH (water) | pH (KCl) | ΔpH |
|---------|------------|----------|-----|
| H-1 | 6.2 | 5.1 | 1.1 |
| H-2 | 6 | 5.7 | 0.3 |
| H-3 | 6.9 | 6.2 | 0.7 |

Specific gravity, void ratio, and dry density: The mineralogy of the dunite residual soils is also reflected in the specific gravity (Gs) of soils, with high Gs values, around 3.2 for the three horizons, compared to the values reported for other fine-grained residual soils in Antioquia (Table 5), with Gs between 2.56 - 2.85.

High values of Gs are associated with high-density minerals, e.g. goethite, hematite, maghemite, and a high degree of laterization (de Graft-Johnson *et al.*, 1972).

Figure 9 shows the variation of specific gravity (Gs), void ratio (e), and dry density with depth. No significant differences were found in the Gs values of the three horizons.

The void ratio was in the range of 1.2 to 1.8 (Figures 9A), which are considered very high values (Brewer, 1964) and increases from H-1 to H-3. These values correspond to an open-texture fabric soil, which added to the existence of cementation, could lead to a collapsible soil typical of non-saturated tropical soils (Fookes, 1997). The dry unit weight shows a behavior contrary to the void ratio, with values between 11.8 kN/m³ and 14.8 kN/m³, decreasing from H-1 to H-3 (Figure 9B).

Table 5. Specific gravity (Gs) of Antioquia’s residual soils.

| Authors | Gs | Residual soil (geological formation) |
|---|------------|--------------------------------------|
| Fresneda-Saldarriaga <i>et al.</i> , 2013 | 2.85 | Amphibolite |
| Romaña <i>et al.</i> , 2009 | 2.6 | Antioquian Batholith |
| Quintero-Ramírez <i>et al.</i> , 2017 | 2.69 | Antioquian Batholith |
| Pineda-Jaimes and Colmenares-Montañez, 2008 | 2.79, 2.81 | Antioquian Batholith |
| Echeverri-Ramírez, 2005 | 2.56, 2.58 | Ovejas Batholith |
| Echeverri-Ramírez, 2005 | 2.65, 2.75 | Altavista Stock |

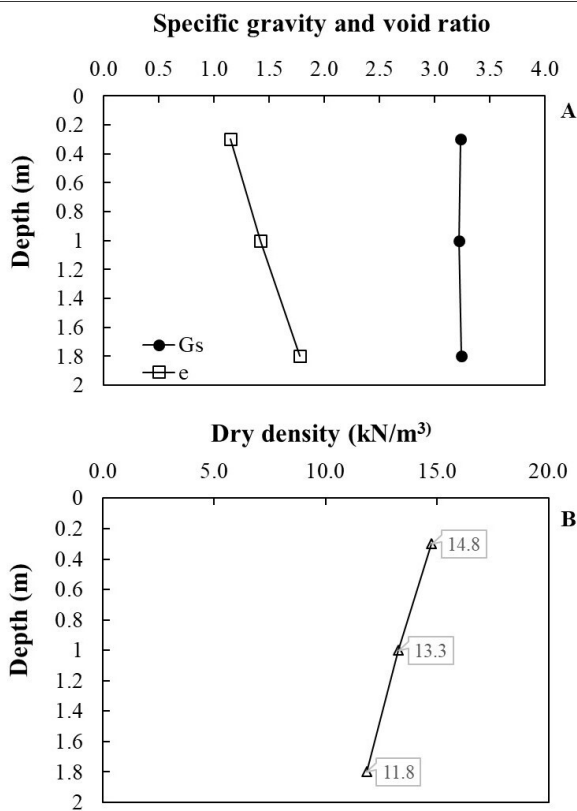


Figure 9. Soil profile and A. Specific gravity and void ratio, B. Dry density.

When evaluating the index properties of the soils and relating them to mineralogy, it was observed that, even though that initially, three soil horizons were defined within the weathering profile (based on macroscopic characteristics). From the point of view of physical-mechanical behavior, the dunite residual soil studied can be divided into two soil horizons: a more superficial horizon H-I with a thickness of 30 cm (ML, lateritic) and a second horizon H-II between 30 cm to 1.8 m deep (MH, not lateritic) made up of the soils initially identified as H-2 and H-3.

Unsaturated-undrained shear strength and stress-strain behavior

The undrained cohesion (C_u) calculated from the UCS test (Table 6), shows that the lateritic horizon (H-1) has a higher shear strength, with $C_u = 98$ kPa and UCS = 196 kPa, and that the resistance values decrease with depth, in the non-lateritic horizons (H-2, H-3).

Table 6. Results of unconfined compressive strength (UCS) test.

| Horizon | Unconfined Compressive Strength, UCS (kPa) | Undrained Cohesion, C_u (kPa) |
|---------|--|---------------------------------|
| H-1 | 196 | 98 |
| H-2 | 128 | 64 |
| H-3 | 55 | 28 |

The same behavior of the undrained shear strength was observed in the results of the UU triaxial test, with $C_u = 92$ kPa in the lateritic horizon (H-1) and lower undrained shear strength in the non-lateritic horizons H-2 and H-3, with C_u between 23 – 30 kPa (Table 7).

Table 7. Parameters of unsaturated - undrained shear strength, UU triaxial test.

| Horizon | Internal friction angle, ϕ° | Undrained Cohesion, C_u (kPa) | Saturation grade (Sr%) |
|---------|---------------------------------------|---------------------------------|------------------------|
| H-1 | 38 | 92 | 72 |
| H-2 | 41 | 23 | 52 |
| H-3 | 30 | 30 | 47 |

An inverse relationship was found between C_u and fines content and plasticity (Figures 10A and 10B).

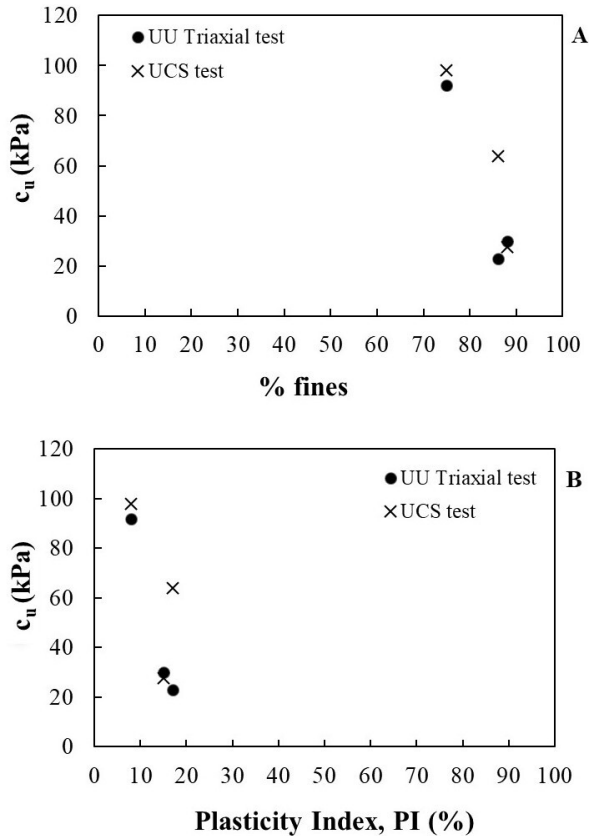


Figure 10. Relationship between undrained cohesion and **A.** fines content, **B.** plasticity index. C_u values from UU triaxial and UCS tests.

The lateritic horizon H-1 had the highest C_u value in both tests (UCS, UU triaxial), and yet it was the horizon with the lowest fines content and the least plasticity, in contrast, the non-lateritic horizons H-2 and H-3 had the lowest C_u value and are the horizons with the highest content of fines and greater plasticity. This behavior can be explained by a higher relative abundance of sesquioxides (hematite and maghemite) in the lateritic horizon H-1, associated with the chemical weathering process. This presence of iron oxides decreases the plasticity of the soil and cements the particles, improving the mechanical properties of the soil, specifically the undrained shear strength of fine-grained soils, due to the electrokinetic precipitation of iron oxide bands (Sowers, 1985; Suárez, 1998; Cundy and Hopkinson, 2005; Larrahondo *et al.*, 2011). Yean-Chin and Chee-Meng (2004) refer to the effect that these binders (goethite, gibbsite, and iron oxides)

generate between the particles, as a kind of apparent cohesion, and that is a component of the shear strength.

UCS and UU triaxial tests were carried out on unsaturated samples, with a saturation degree $S_r = 72\%$ in H-1 and decreasing with depth to $S_r = 47\%$ in H-3. The undrained cohesion (C_u) values determined with these tests might have a contribution from suction because the soils were in a non-saturated condition, however, this aspect was not evaluated in the present research.

The friction angle was similar for horizons H-1 and H-2 (38° and 41°) and decreased to 30° for horizon H-3. These friction angles are very high, compared to the friction angle of lateritic clays derived from amphibolite ($\phi = 10^\circ$) (Fresneda-Saldarriaga *et al.*, 2013) and the residual soils of the Antioquian Batholith ($\phi = 23^\circ$) (Romaña *et al.*, 2009), and similar to the values reported for other lateritic soils with friction angles between $28^\circ - 39^\circ$ (Suárez, 1998).

Figure 11 corresponds to the stress-strain curve for a confining pressure of 50 kPa, 100 kPa, and 200 kPa, obtained from the UU triaxial test. It shows that for a 50 kPa of confining pressure, the lateritic horizon H-1, reaches the peak strength (580 kPa) at the low strain range, and shearing continued until the ultimate strength was obtained, or fully softened (450 kPa) at larger strain. This soil exhibits a brittle failure. For higher confining pressures (100 and 200 kPa) lateritic horizon H-1 presents a ductile failure, as do horizons H-2 and H-3 at all confining pressures, since the strength only increases with strain, no peak, and no strain softening. This behavior is typical of normally consolidated clay and uncemented soil.

Based on the present results it can be affirmed that the presence of minerals like goethite, as the main contributor, gibbsite, maghemite, and hematite, less abundant, are playing the role of bonding to the phyllosilicates (kaolinite, talc, clinocllore) of the dunite residual soils. In this sense, it could be hypothesized that phyllosilicates, due to their layered structure, possess a high potential of generating slide surfaces through these planes and abruptly collapse, when the resistance, provided by the oxide and oxyhydroxide bonds, is destroyed.

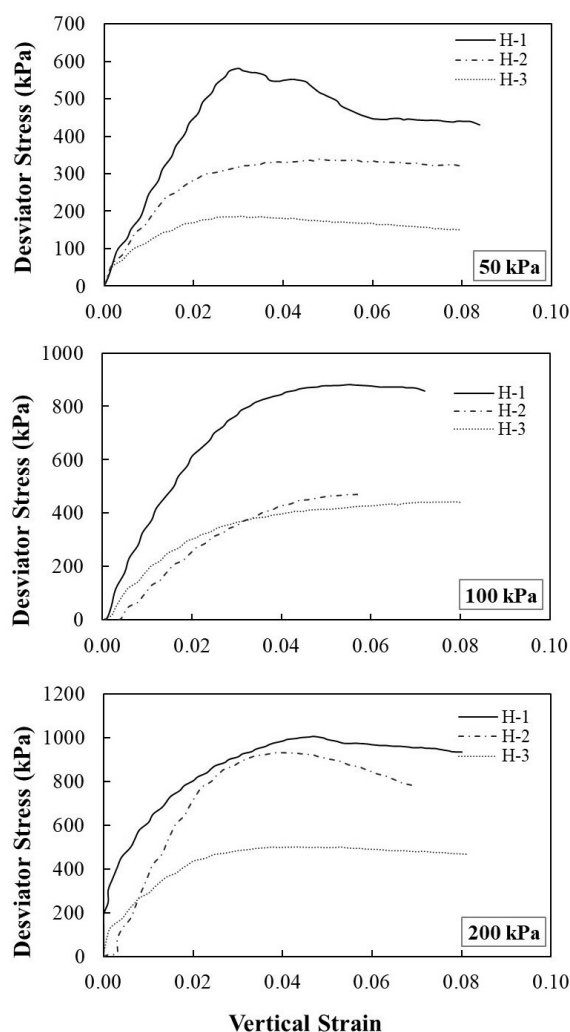


Figure 11. Stress-Strain curve at 50, 100, 200 kPa of confining pressure of Medellín Dunite residual soils.

Conclusions

The residual soils studied are the result of the weathering process of the Medellín Dunite. The results show a relationship between the physical properties and the undrained shear strength of these soils with mineralogy.

In the study area, initially, three soil horizons were identified macroscopically on a slope cut, however, based on the mineralogical and physical-mechanical characterization, it is concluded that the dunite residual soils present two weathering horizons with marked differences in their geotechnical behavior.

The most shallow soils are between 0.00 – 0.30 m, corresponding to a lateritic silt horizon (H-I) with a lower

fines content and less plasticity. Their higher relative content of iron oxi-hydroxides, goethite, aluminum hydroxides, gibbsite, and iron oxides, hematite, and maghemite, act as cementitious bonds for the soil matrix, generating higher unconfined compressive strength (UCS), greater undrained cohesion (C_u) and undrained shear strength and exhibit brittle failure at low confining pressure (50 kPa). Underlain by a non-lateritic silt horizon (H-II) between 0.30 – 1.80 m, with a higher fines content and a more remarkable plasticity, but, the lower relative abundance of the minerals described above, leading to lower UCS and C_u , with ductile failure, a behavior typical of uncemented soils.

The findings of this study agree with [Yean-Chin and Chee-Meng \(2004\)](#) and [Wesley \(2010\)](#), on the central role of oxi-hydroxides as cementing agents, responsible for an apparent cohesion in soils.

For a complete understanding of Medellín Dunite residual soils, it is necessary to continue this research including other aspects. For example, path compressibility under load, soil microstructure focusing on the distribution of oxides and oxi-hydroxides in the soil matrix, and contribution of suction to undrained cohesion. The results have limitations concerning the soil sampling method, which could have altered/destroyed the cementation of the soils and the number of samples and tests that represent each horizon.

Acknowledgements

In Memoriam of Michel Hermelín Arbaux (1937-2015). Professor Hermelín, people like you never die because your genius will be forever present in our minds and your kindness in our hearts.

The authors are grateful to Laboratorio de Biomineralogía y Biohidrometalurgia (Universidad Nacional de Colombia-Sede Medellín), to the Dirección de Investigación y Posgrados del Politécnico Colombiano Jaime Isaza Cadavid and project “Influencia de la mineralogía en el comportamiento mecánico de suelos in-situ derivados de la Dunite de Medellín”, and to Posgrado en Geotecnia de la Universidad de Brasilia (Brazil). ALM is grateful to: CODI-Universidad de Antioquia (Estrategia de Sostenibilidad de la Universidad de Antioquia and projects “Propiedades magneto-ópticas y óptica no lineal en superredes de Grafeno”, “Estudio de propiedades ópticas en sistemas semiconductores de dimensiones nanoscópicas”, and “Propiedades

de transporte, espintrónicas y térmicas en el sistema molecular zinc-porfirina”), and Facultad de Ciencias Exactas y Naturales-Universidad de Antioquia (ALM exclusive dedication project 2021-2022). ALM also acknowledges the financial support from El Patrimonio Autónomo Fondo Nacional de Financiamiento para la Ciencia, la Tecnología y la Innovación Francisco José de Caldas (project: CD111580863338, CT FP80740-173-201).

References

- Álvarez-Agudelo, J. (1987). Tectonitas Dunitas de Medellín, Departamento de Antioquia, Colombia. *Boletín Geológico*, 28(3), 9-44.
- Araki, M.S. (1997). Aspectos relativos às propriedades dos solos porosos colapsíveis do Distrito Federal. Dissertação de Mestrado em Geotecnia, Universidade de Brasília, Brasil.
- ASTM D2216-19. Standard Test Method for Laboratory Determination of Water (Moisture) Content of Soil and Rock by Mass. ASTM International, West Conshohocken, PA, 2019. <https://doi.org/10.1520/D2216-19>
- ASTM D854-14. Standard Test Methods for Specific Gravity of Soil Solids by Water Pycnometer. ASTM International, West Conshohocken, PA, 2014. <https://doi.org/10.1520/D0854-14>
- ASTM D4318-17e1. Standard Test Methods for Liquid Limit, Plastic Limit, and Plasticity Index of Soils. ASTM International, West Conshohocken, PA, 2017. <https://doi.org/10.1520/D4318-17E01>
- ASTM D422-63(2007)e1. Standard Test Methods for Particle-Size Analysis of Soils. ASTM International, West Conshohocken, PA, 2007. <https://doi.org/10.1520/D0422-63R07E01>
- ASTM D2487-17e1. Standard Practice for Classification of Soils for Engineering Purposes (Unified Soil Classification System). ASTM International, West Conshohocken, PA, 2017. <https://doi.org/10.1520/D2487-17E01>
- ASTM D2166-16. Standard Test Method for Unconfined Compressive Strength of Cohesive Soil. ASTM International, West Conshohocken, PA, 2016. https://doi.org/10.1520/D2166_D2166M-16
- ASTM D2850-15. Standard Test Method for Unconsolidated-Undrained Triaxial Compression Test on Cohesive Soils. ASTM International, West Conshohocken, PA, 2015. <https://doi.org/10.1520/D2850-15>
- Bo, M.W.; Aruljarah, A.; Sukmak, P.; Horpibulsuk, S. (2015). Mineralogy and geotechnical properties of Singapore marine clay at Changi. *Soils and Foundations*, 55(3), 600-613. <https://doi.org/10.1016/j.sandf.2015.04.011>
- Brewer, R. (1964). *Fabric and mineral analysis of soils*. Wiley & Sons.
- Cundy, A.B.; Hopkinson, L. (2005). Electrokinetic iron pan generation in unconsolidated sediments: implications for contaminated land remediation and soil engineering. *Applied Geochemistry*, 20(5), 841-848. <https://doi.org/10.1016/j.apgeochem.2004.11.014>
- de Graft-Johnson, J.W.S.; Bhatia, H.; Hammond, A.A. (1972). Lateritic gravel evaluation for road construction. *Journal of the Soil Mechanics and Foundations Division*, 98(11), 1245-1265. <https://doi.org/10.1061/JSFEAQ.0001806>
- Deere, D.; Patton, F. (1971). Slope stability in residual soils. *4th Pan American Conference on Soil Mechanics and Foundation Engineering*, San Juan, Puerto Rico.
- Echeverri-Ramírez, O. (2005). Efecto de la microestructura en los parámetros de resistencia al esfuerzo cortante de algunos suelos provenientes de rocas ígneas presentes en Medellín. M.Sc. Tesis, Universidad Nacional de Colombia, Medellín, Colombia.
- Fookes, P. (1997). *Tropical Residuals Soils*. Geological Society Professional Handbook.
- Fresneda-Saldarriaga, C.; Navarro-Saldarriaga, S.; Valencia-González, Y. (2013). Caracterización geotécnica de un suelo tropical laterítico. *INGE CUC*, 9(1), 219-230.
- García-Casco, A.; Restrepo, J.J.; Correa-Martínez, A.M.; Blanco-Quintero, I.F.; Proenza, J.A.; Weber, M.; Butjosa, L. (2020). The petrologic nature of the “Medellín Dunite” revisited: An algebraic approach and proposal of a new definition of the geological body. In: J. Gómez, A.O. Pinilla-Pachon (ed.). *The Geology of Colombia* (pp. 45-75), Volume 2, Servicio

- Geológico Colombiano. <https://doi.org/10.32685/pub.esp.36.2019.02>
- Gidigasú, M.D. (1972). Mode of formation and geotechnical characteristic of laterite materials of Ghana in relation to soil forming factor. *Engineering Geology*, 6(2), 79-150. [https://doi.org/10.1016/0013-7952\(72\)90034-8](https://doi.org/10.1016/0013-7952(72)90034-8)
- Kiehl, E. (1979). *Manual de Edafología: Relações Solo – Planta*. Editora Agronômica “CERES” Ltda.
- Lagarec, K.; Rancourt, D.G. (1998). Mössbauer Spectral Analysis Software for Windows, version 1.0. Department of Physics, University of Ottawa, 1-40.
- Larrahondo, J.M.; Choo, H.; Burns, S.E. (2011). Laboratory-prepared iron oxide coatings on sands: Submicron-scale small-strain stiffness. *Engineering Geology*, 121(1-2), 7-17. <https://doi.org/10.1016/j.enggeo.2011.04.009>
- Little, A.L. (1969). The engineering classification of residual tropical soils. *7th International Conference of Soil Mechanics and Foundation Engineering*, México city, México.
- Morales, A.L. (2003). An X-ray diffraction study of corrosion products from low carbon steel. *Revista de Metalurgia*, 39(Extraordinario 1), 28-31.
- National Engineering Handbook. (2021). Part 650 Engineering Field Handbook. Elementary Soil Engineering Chapter 4. United States Department of Agriculture, NRCS.
- Nogami, J.S.; Villibor, D.F. (1994). Identificação expedita dos grupos de classificação MCT para solos tropicais. *X Congresso Brasileiro de Mecânica de Suelos e Ingeniería de Fundaciones*, São Paulo, Brasil.
- Pineda-Jaimes, J.A.; Colmenares-Montañez, J.E. (2008). Efectos de la meteorización en las propiedades de retención de humedad de dos suelos residuales derivados de una granodiorita. *Épsilon*, 1(10), 9-21.
- Quintero-Ramírez, A.; Valencia-González, Y.; Lara-Valencia, L.A. (2017). Variaciones geotécnicas en un suelo tropical causadas por los lixiviados de residuos sólidos urbanos: Escala laboratorio. *Boletín de Ciencias de la Tierra*, 41, 40-47. <https://doi.org/10.15446/rbct.n41.57876>
- Rahardjo, H.; Aung, K.K.; Leong, E.C.; Rezaur, R.B. (2004). Characteristics of residual soils in Singapore as formed by weathering. *Engineering Geology*, 73(1-2), 157-169. <https://doi.org/10.1016/j.enggeo.2004.01.002>
- Rodríguez, G.; González, H.; Zapata, G. (2005). Geología de la plancha 147 Medellín Oriental. INGEOMINAS. Comprende mapa a escala 1:50.000 e informe, 312 p.
- Romaña, J.F.; Zapata, G.; Giraldo, R.; Valencia, Y. (2009). Efecto de la meteorización en el comportamiento de un suelo tropical del oriente antioqueño. *XV Jornadas Geotécnicas de la Ingeniería Colombiana*, Bogotá, Colombia.
- Serna-Quintana, C.A. (2011). La naturaleza social de los desastres asociados a inundaciones y deslizamientos en Medellín (1930-1990). *Historia Crítica*, 43, 198-223. <https://doi.org/10.7440/histcrit43.2011.11>
- Shaour, F.M.; Jarrar, G.; Hencher, S.; Kuisi, M. (2008). Geotechnical and mineralogical characteristics of marl deposits in Jordan. *Environmental Geology*, 55(8), 1777-1783. <https://doi.org/10.1007/s00254-007-1128-5>
- Sowers, G.F. (1985). Residual Soils in the United States. In: E.W. Brand, H.B. Phillipson (eds.). *Sampling and Testing of Residual Soils. A Review of International Practice* (pp. 183-191). Scorpion Press.
- Suárez, J. (1998). *Deslizamientos y estabilidad de taludes en zonas tropicales*. Publicaciones UIS.
- Tsige, M.; González de Vallejo, L. (1996). Microfábrica de las arcillas azules del Guadalquivir y su relación con los procesos de meteorización. *Geogaceta*, 20(6), 1324-1327.
- Wesley, L.D. (2010). *Geotechnical Engineering in Residual Soils*. Wiley & Sons, Inc.
- Yean-Chin, T.; Chee-Meng, C. (2004). Slope stability and stabilization. In: B.B.K. Huat, G. See-Sew, F.H. Ali (eds.). *Tropical Residual Soils Engineering* (pp. 169-192). Taylor & Francis Group.

Received: 29 April 2021

Accepted: 04 October 2022
